

PHYSICAL REVIEW LETTERS

VOLUME 63

6 NOVEMBER 1989

NUMBER 19

Crossover Scaling from Multifractal Theory: Dielectric Breakdown with Cutoffs

Eyal Arian,^(1,2) Preben Alstrøm,⁽¹⁾ Amnon Aharony,^(2,3) and H. Eugene Stanley⁽¹⁾

⁽¹⁾Center for Polymer Studies and Department of Physics, Boston University, Boston, Massachusetts 02215

⁽²⁾School of Physics and Astronomy, Beverly and Raymond Sackler Faculty of Exact Sciences,
Tel Aviv University, Tel Aviv 69978, Israel

⁽³⁾Institute of Physics, University of Oslo, Oslo, Norway

(Received 15 May 1989)

The dielectric breakdown model (DBM) is generalized to include lower cutoffs, which prevent growth at low fields. The new models may represent realistic situations in some DBM and some viscous fingering experiments. Multifractal theory is shown to provide quantitative predictions for the crossover from the usual DBM patterns (at small finger sizes) to a new, spiky, behavior (at large sizes). For one of the models, the theory also predicts when growth will stop. The predicted crossover scaling function is confirmed by numerical simulations.

PACS numbers: 05.40.+j, 02.50.+s, 47.60.-i, 52.80.-s

Much of the recent interest in fractal growth phenomena^{1,2} has arisen because of the *universal* nature of the observed patterns: viscous fingering in porous media,³ dielectric breakdown,⁴ diffusion-limited electrodeposition or growth in aqueous solutions,^{5,6} and diffusion-limited aggregates⁷ all give rise to similar structures. A zeroth-order approximation to these phenomena is provided by the dielectric breakdown model⁴ (DBM): One solves the Laplace equation $\nabla^2\phi=0$ in the medium surrounding the growing aggregate, with the boundary conditions $\phi=0$ on the aggregate and $\phi=1$ on the surrounding (distant) boundary; one calculates the gradients of ϕ normal to the boundary, $\nabla_i = |(\nabla\phi)_i| \equiv |(\mathbf{n}\cdot\nabla\phi)_i|$ at the point i on the boundary; and then one stochastically moves the boundary at point i with probability

$$p_i \equiv \frac{\nabla_i^\eta}{\sum_i \nabla_i^\eta}. \quad (1)$$

For $\eta=1$, in two space dimensions the resulting aggregates have a fractal dimension $D \approx 1.7$, and look the same as many of the above observed phenomena, *irrespective of details*. For $\eta=0$, the results reproduce the Eden growth model.⁸ The above two cases correspond to real viscous fingers for fast and slow flow rates, respectively.⁹

The fact that η uniquely identifies the universality classes of DBM makes η analogous to parameters like n ,

the number of spin components, or σ , the power of the decay of long-range interactions, in critical phenomena.¹⁰ As in critical phenomena, one would thus expect a *crossover* between different universality classes to occur whenever there exist competing interactions. For example, a competition between the viscous and the capillary forces might result in a crossover between the patterns with $\eta=1$ and 0.⁹ In this Letter we show that *such crossover phenomena do indeed occur*. Moreover, we study the simplest examples of such a crossover and find, to our surprise, that the theory of *multifractal scaling*¹¹ can yield *analytic predictions* for details of the crossover.

We study two models. In “model I,” we assume that the $\{p_i\}$ have a lower cutoff, p_c , so that there is no growth at point i if $p_i \leq p_c$. The rest of the probabilities are renormalized by $p' \equiv \sum_{p_i > p_c} p_i$ (i.e., $p_i \rightarrow p_i/p'$). This is a model where the pattern stops growing, as actually happens in some DBM experiments.¹² In “model II,” the cutoff is on the gradients; i.e., there is no growth at point i if $\nabla_i \leq \nabla_c$. Since the denominator in Eq. (1) has a nontrivial dependence on the size of the aggregate (see below), the two models have very different behavior.

Model II has two physical motivations. The first is the introduction of a critical field, E_c , as a breakdown criterion¹² in the DBM. It was noted recently¹³ that such a criterion leads to a crossover of the dielectric breakdown pattern, when the pattern reaches a crossover radius R_x

(which depends on E_c). Our analysis yields an explicit *analytic* expression for the dependence of R_x on E_c , which differs from that conjectured (for the same model) in Ref. 13. It would be very interesting to check this dependence [Eq. (19) below] experimentally.

The second physical motivation is the introduction of a capillary pressure into the problem of viscous fingering. If the displacement is of a wetting fluid by a nonwetting fluid, then the capillary pressure prevents the nonwetting phase to enter a pore when the pressure is lower than the local capillary pressure P_c .¹⁴ In simulations of porous media as a network of ducts,¹⁴ P_c depends only on the ducts' width via the Laplace law. Taking the radii of the ducts to be constant all over the network, we conclude that each bond will be active if the viscous pressure on it, P , is bigger than P_c , and will not be active if $P < P_c$. We see that the capillary pressure is the equivalent of the critical field, and both are represented by V_c in model II. The crossover effects discussed here are expected in experiments done at constant flow rate and may be absent in experiments done at constant pressure. For technical reasons, to be explained below, we find it easier to demonstrate the essential new crossover phenomena in model I, and then discuss our predictions for model II.

In order to understand the crossovers we consider the exponents¹⁵

$$\alpha_i \equiv -\ln p_i / \ln R, \quad (2)$$

where R is the radius of gyration of the cluster, and p_i are the growth probabilities for that particular cluster. The exponents α_i are bounded from below by

$$\alpha_{\min} \equiv -\ln p_{\max} / \ln R, \quad (3)$$

where p_{\max} is the maximum probability. The total number of perimeter sites N is divided into subsets N_α , where $N_\alpha \Delta\alpha$ is the number of sites i with $\alpha \leq \alpha_i < \alpha + \Delta\alpha$. From *multifractal theory* each of these numbers N_α scales with R ,

$$N_\alpha \propto R^{f(\alpha)}, \quad (4)$$

which defines the function $f(\alpha)$. It is possible to reliably calculate $f(\alpha)$ by averaging over several aggregates at least for $\alpha \leq 1$.¹⁵

Based on this distribution we now calculate the probability $P(\alpha)$ that the growth takes place on some site characterized by the exponent α . Since there are $N_\alpha \propto R^{f(\alpha)}$ such points, each having growth probability $p_\alpha \propto R^{-\alpha}$, we find

$$P(\alpha) = N_\alpha p_\alpha \propto R^{f(\alpha) - \alpha}. \quad (5)$$

This is maximal when $f(\alpha) = 1$, which defines a value $\alpha = \alpha_I$. However, since $\sum_\alpha P(\alpha) = 1$, $f(\alpha) \leq \alpha$, which implies that in the scaling limit ($R \rightarrow \infty$)

$$P(\alpha) \rightarrow \delta(\alpha - \alpha_I). \quad (6)$$

Thus, by definition $f(\alpha_I) = \alpha_I$ equals the information dimension D_I for the harmonic measure, which for connected sets in 2D is generally accepted to be^{2,16} $D_I = 1$.

Consider now model I. Since practically all growth takes place on sites with probability $p_I \propto R^{-\alpha_I} = R^{-1}$, the usual DBM-type growth is not affected before p_I reaches the cutoff value p_c . Our analysis therefore predicts that the crossover takes place when $p_I \approx p_c$, i.e., when the cluster radius reaches a crossover value

$$R_x \propto p_c^{-1}. \quad (7)$$

To test the prediction (7), we produced several DBM aggregates with the model-I cutoff. For each value of p_c we (at given values of R) found the average mass $M(R)$ over twenty aggregates. We performed simulations with $\eta = 1$, on a square lattice, and the external boundary was set on a circle at radius $L = 100$. The solution to Laplace's equation was determined with a relative accuracy of 1%, and the growth of the aggregate was stopped when it became close to the external boundary ($R/L \approx 90\%$). Examples of the growing aggregates are shown in Fig. 1. For very small p_c ($p_c < 0.002$ in our example), we observe only the usual DBM structure, with $D \approx 1.7$ [Fig. 1(a)]. For intermediate values of p_c , there is a crossover to a spiky structure, with $D = 1$ [Fig. 1(b)], for radii larger than a crossover radius, R_x . After the crossover, the growth is in a narrow regime of probabilities between p_c and p_{\max} , which corresponds to growing

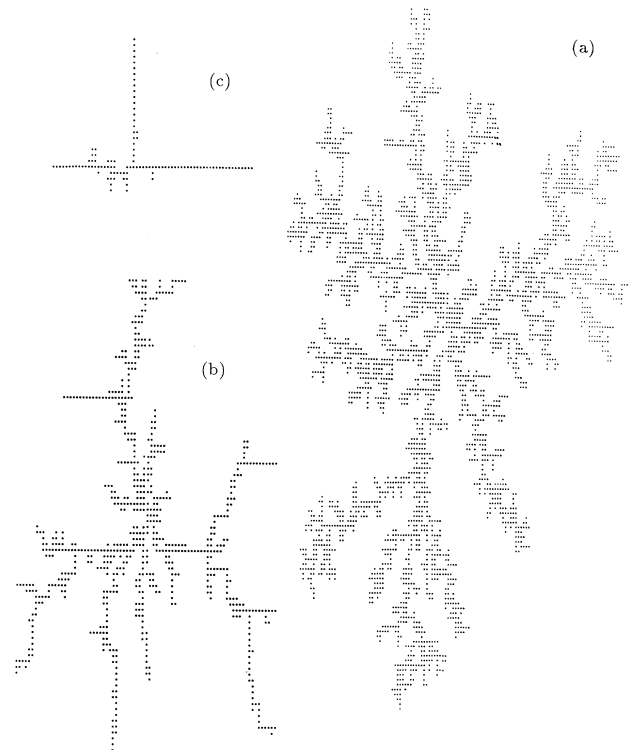


FIG. 1. Dielectric breakdown patterns with a growth probability threshold p_c . (a) $p_c = 0.001$. The aggregate looks like the usual DBM aggregate ($p_c = 0$). (b) $p_c = 0.006$. A crossover from the usual DBM structure to a spiky structure is apparent. (c) $p_c = 0.06$. The growth stops before the aggregate hits the boundary.

on the tips. The spiky structure corresponds to $\eta = \infty$, when only one tip grows, and the growth of the aggregate was stopped when it became close to the external boundary ($R/L \approx 90\%$). For larger values of p_c , all the p_i became smaller than p_c even before the aggregate got close to the boundary (in our example this happens for $p_c > 0.02$). In this case growth stops [Fig. 1(c)] at a finite radius R_{\max} .

With p_c in the range $0.002 < p_c < 0.02$, we observe a crossover. For $R < R_x$, the mass scales with R according to the mass dimension for the usual DBM structure, i.e.,

$$M(R) \propto R^D, \quad (8)$$

where $D \approx 1.7$. Above R_x , $M(R)$ approaches a linear dependence on R . This behavior is in accordance with the spiky structure above the crossover, and $M(R)$ can be well approximated by the simple behavior

$$M(R) \propto \begin{cases} R^D, & \text{if } R < R_x, \\ R_x^D + A(R - R_x), & \text{if } R > R_x, \end{cases} \quad (9)$$

where A depends on R_x . Changing p_c changes the value of R_x . Next we plot $\mathcal{F} \equiv M(R)R^{-D}$ against $x \equiv Rp_c$, with $D=1.7$, for different p_c values [Fig. 2(a)]. The good data collapse shows that the simulations are in agreement with the theoretical prediction (7). The deviations at maximal R values ($R \approx 100$) are due to boundary effects not included in the scaling function $\mathcal{F}(x)$.

In the crossover region, the mass of the aggregate can be fitted by a *universal crossover function*,

$$M(R) = R^D \mathcal{F}(Rp_c), \quad (10)$$

as shown in Fig. 2. From (9) we conclude that the scaling function $\mathcal{F}(x)$ has the form

$$\mathcal{F}(x) = \begin{cases} \text{const}, & \text{if } x < x_c, \\ (ax + b)x^{-D}, & \text{if } x > x_c, \end{cases} \quad (11)$$

where the constant is found from Fig. 2(a) to be ≈ 3.1 . To determine a and b we have in Fig. 2(b) plotted $\mathcal{F}(x)x^D$, i.e., $Mp_c^{1.7}$ vs $x \equiv Rp_c$. We find $a \approx 0.62$ and $b \approx -0.014$; hence $x_c \equiv R_x p_c \approx 0.05$. The deviations from the straight line for large x [Fig. 2(b)] arise again from boundary effects. We emphasize, however, that although boundary effects are present for radii well below the radius of the final cluster ($R/L \approx 90\%$), these effects are not important at R_x . This is especially clear in Fig. 2(b), where no boundary effects are apparent for $x < 0.25$, which is to be compared with the 5 times smaller value of x_c defined above.

Consider further the behavior for $R > R_x$, where the fractal DBM nature is broken leaving a one-dimensional spiky structure. If the boundary is sufficiently far away, the growth continues until p_{\max} reaches p_c . To find where the growth stops, i.e., to find $R_{\max}(p_c)$, we must therefore find the behavior of

$$p_{\max} \equiv \frac{\mathbf{V}_{\max}}{\sum_i \mathbf{V}_i}, \quad (12)$$

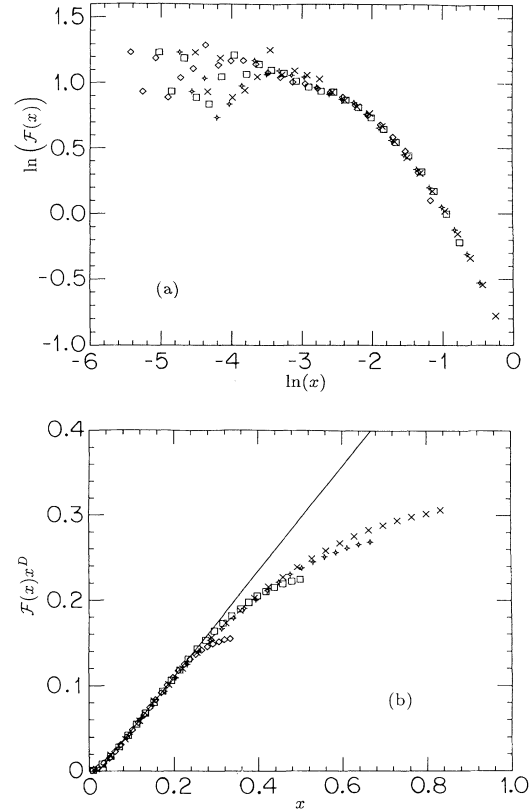


FIG. 2. (a) Scaling function $\mathcal{F} \equiv MR^{-D}$ vs $x \equiv Rp_c$, where $D=1.7$. The plot is double logarithmic in order to magnify the crossover region. (b) $\mathcal{F}(x)x^D \equiv Mp_c^{1.7}$ vs $x \equiv Rp_c$. The straight line $ax + b$ has $a = 0.62$ and $b = -0.014$. Four values of p_c are shown: 0.004 (diamond), 0.006 (square), 0.008 (plus), and 0.010 (cross).

where \mathbf{V}_{\max} is the maximal gradient, $\mathbf{V}_{\max} \equiv \max_i \{\mathbf{V}_i\}$. Note that only the denominator scales, while \mathbf{V}_{\max} is always of order 1.¹⁷ Hence,

$$\sum_i \mathbf{V}_i \propto R^{\alpha_{\min}}. \quad (13)$$

When the mass M grows to $M + 1$, this sum changes by

$$\frac{\Delta \sum_i \mathbf{V}_i}{\Delta M} = \frac{\Delta \sum_i \mathbf{V}_i / \Delta R}{\Delta M / \Delta R} \propto R^{\alpha_{\min} - D}. \quad (14)$$

Reaching R_x , this derivative has a value $\propto p_c^{D - \alpha_{\min}}$. Furthermore, a growth on a spiky tip does not influence this derivative, which approximately stays equal to the derivative at the bottom of the spike, i.e., at the crossover. We conclude that above the crossover, $\sum_i \mathbf{V}_i$ increases linearly with mass. Since the mass increases linearly with size,

$$p_{\max} \propto p_c^{\alpha_{\min} - D} R^{-1}. \quad (15)$$

At $R = R_{\max}$, $p_{\max} \approx p_c$, which gives

$$R_{\max} \propto p_c^{\alpha_{\min} - D - 1}. \quad (16)$$

Adopting¹⁸ $\alpha_{\min} = D - 1$,

$$R_{\max} \propto p_c^{-2}. \quad (17)$$

In our numerical simulations, we find systematic deviations from Eq. (17) when the growth stops too close to the boundary. There were too few values of p_c for which this did not happen, and therefore we were unable to obtain an accurate check of (17). Forcing all the data into $R_{\max} \propto p_c^{-s}$ yields $s = 2.2 \pm 0.2$.

In model II, the crossover is imposed by a cutoff in the gradient: There is no growth if $\nabla_i \leq \nabla_c$, and the "surviving" probabilities are renormalized, $p_i \rightarrow p_i/\hat{p}$, where $\hat{p} \equiv \sum_{\nabla_i > \nabla_c} p_i$. Unlike model I, the growth will not stop (before the boundary), since ∇_{\max} is of order 1.¹⁷ Here, the scaling analysis predicts the crossover to occur at a distance R_x where

$$\nabla_I \equiv p_I \sum_i \nabla_i \quad (18)$$

reaches ∇_c . Using (13), $D_I = 1$, and $\alpha_{\min} = D - 1$, we obtain

$$R_x \propto \nabla_c^{-1/(2-D)}. \quad (19)$$

For the DBM, where $D \approx 1.7$, the exponent in (19) is ≈ 3 . This means that the region where the crossover is apparent is predicted to be much smaller for the gradient cutoff than for the probability cutoff. We have performed simulations for various values of ∇_c . Our results show the range of values of ∇_c in which the crossover is apparent (for the crossover from the usual DBM structure to a spiky structure) is indeed much narrower. For this reason we have not been able to measure a reliable numerical value of the crossover exponent. Furthermore, for small values of ∇_c we observe a wide range of radii, where the produced patterns are neither DBM-like nor spiky. This is, however, consistent with a description of model II in terms of a crossover function \mathcal{G} , i.e., $M(R) = R^D \mathcal{G}(R \nabla_c^{1/(2-D)})$. Since the exponent $1/(2-D)$ is large, a small variation of R for large values of ∇_c corresponds to a very large variation of R for small values of ∇_c . This effect makes the detection of the crossover radius and the associated exponent difficult. In contrast, the crossover exponent in model I is 1, which makes the numerical determination of the crossover easier.

In the context of viscous fingering in porous media, model II suggests that the DBM structure may eventually cross over to a spiky structure at low pressure. In particular, in relation to the phase diagram proposed by Lenormand and co-workers¹⁴ we speculate that even for small viscosity ratio, the DBM structure will eventually cross over to a spiky pattern.

In conclusion, we have treated the crossover phenomenon in DBM imposing a cutoff p_c in the probability (model I) or ∇_c in the gradient (model II). We have shown the existence of a crossover from the usual DBM-type to a spiky-type aggregate, i.e., the crossover from

$\eta = 1$ to the $\eta = \infty$ universality class. For the probability cutoff we find that this crossover takes place at a distance $R_x(p_c) \propto p_c^{-1}$, while the growth continues to a distance $R_{\max}(p_c) \propto p_c^{-2}$ when boundary effects can be neglected. For the gradient cutoff we find the crossover radius to scale according to $R_x(\nabla_c) \propto \nabla_c^{-1/(2-D)}$.

The exponents can be understood from multifractal analysis, based on the equations $D_I = 1$ and $\alpha_{\min} = D - 1$, where the latter equation is believed to be of general nature, e.g., valid for all η . For general η we find $R_x(p_c) \propto p_c^{-1/D_I}$, $R_{\max}(p_c) \propto p_c^{-(1+1/D_I)}$ for model I. For model II, the crossover exponent is $1/(D_I + 1 - D)$. In particular, all exponents diverge in the $\eta = \infty$ limit ($D = 1$, $D_I = 0$).

The observation that p_I dominates the growth in the scaling limit suggests a general way of obtaining exponents for crossover phenomena similar to those described above. Thus, although our new description is applied to simple models, we believe that it can be taken much further to explain a number of observed crossover phenomena. To this end we urge, in particular, more experimental studies.

The Center for Polymer Studies is supported by grants from NSF and ONR. We also acknowledge support from the Carlsberg Foundation, the Danish Natural Science Research Council, the Israeli Academy of Sciences and Humanities, and the U.S.-Israeli Binational Science Foundation.

¹B. Mandelbrot, *The Fractal Geometry of Nature* (Freeman, San Francisco, 1982).

²J. Feder, *Fractals* (Plenum, New York, 1988); T. Vicsek, *Fractal Growth Phenomena* (World Scientific, Singapore, 1989).

³J. Nittmann, G. Daccord, and H. E. Stanley, *Nature* (London) **314**, 141 (1985); K. J. Måløy, J. Feder, and T. Jøssang, *Phys. Rev. Lett.* **55**, 2688 (1985).

⁴L. Niemeyer, L. Pietronero, and H. J. Wiesmann, *Phys. Rev. Lett.* **52**, 1033 (1984).

⁵M. Matsushita, M. Sano, Y. Hayakawa, H. Honjo, and Y. Sawada, *Phys. Rev. Lett.* **53**, 286 (1984).

⁶Y. Sawada, A. Dougherty, and J. P. Gollub, *Phys. Rev. Lett.* **56**, 1260 (1986).

⁷T. A. Witten and L. M. Sander, *Phys. Rev. Lett.* **47**, 1400 (1981).

⁸P. Meakin, in *On Growth and Form*, edited by H. E. Stanley and N. Ostrowsky (Martinus Nijhoff, Dordrecht, 1985), p. 111; M. Eden, in *Proceedings of the Fourth Berkeley Symposium on Mathematics, Statistics and Probability, Berkeley, California, 1960*, edited by J. Neyman (Univ. of California Press, Berkeley, 1961), Vol. 4, p. 223.

⁹U. Oxaal, M. Murat, F. Boger, A. Aharony, J. Feder, and T. Jøssang, *Nature* (London) **329**, 32 (1987).

¹⁰See, e.g., A. Aharony, in *Phase Transitions and Critical Phenomena*, edited by C. Domb and M. S. Green (Academic, New York, 1976), Vol. 6, p. 357.

¹¹See, e.g., the recent elementary review by B. Mandelbrot, in *Random Fluctuations and Pattern Growth: Experiments and*

Models, edited by H. E. Stanley and N. Ostrowsky (Kluwer, Dordrecht, 1988), p. 333, and references therein.

¹²H. J. Wiesmann and H. R. Zeller, *J. Appl. Phys.* **60**, 1770 (1986).

¹³L. Pietronero and H. J. Wiesmann, *Z. Phys. B* **70**, 87 (1988).

¹⁴R. Lenormand and C. Zarcone, *Phys. Rev. Lett.* **54**, 2226 (1985); R. Lenormand, *Physica (Amsterdam)* **140A**, 114 (1986); R. Lenormand, E. Touboul, and C. Zarcone, *J. Fluid Mech.* **189**, 165 (1988).

¹⁵C. Amitrano, A. Coniglio, and F. di Liberto, *Phys. Rev. Lett.* **57**, 1016 (1986).

¹⁶T. C. Halsey, P. Meakin, and I. Procaccia, *Phys. Rev. Lett.*

56, 854 (1986), and references therein.

¹⁷Actually, V_{\max} increases slightly with size. However, since $V_{\max} < 1$, it cannot scale as $V_{\max} \propto R^y$ with a positive exponent y . Thus $y = 0$, and V_{\max} is of order 1.

¹⁸This statement follows since

$$\begin{aligned} \Delta R / \Delta M &= R(M+1) - R(M) \\ &= p_{\max}[R(M)+1] + (1-p_{\max})R(M) - R(M) \\ &= p_{\max}, \end{aligned}$$

and $\Delta R / \Delta M = 1 / (\Delta M / \Delta R) \propto R^{1-D}$ [L. Turkevich and H. Scher, *Phys. Rev. Lett.* **55**, 1026 (1985)].